PLOS ONE

RESEARCH ARTICLE

Integration of *in vitro* and *in silico* perspectives to explain chemical characterization, biological potential and anticancer effects of *Hypericum salsugineum*: A pharmacologically active source for functional drug formulations

Onur Bender[1], Eulogio J. Llorent-Martínez[2], Gokhan Zengin[3]*, Adriano Mollica[4], Ramazan Ceylan[3], Lucia Molina-García[2], Maria Luisa Fernández-de Córdova[2], Arzu Atalay[1]*

1 Biotechnology Institute, Ankara University, Ankara, Turkey, **2** Department of Physical and Analytical Chemistry, University of Jaén, Campus Las Lagunillas S/N, Jaén, Spain, **3** Deparment of Biology, Science Faculty, Selcuk University, Campus, Konya, Turkey, **4** Department of Pharmacy, University "G. d'Annunzio" of Chieti-Pescara, Chieti-Italy

* gokhanzengin@selcuk.edu.tr (GZ); arzu.atalay@ankara.edu.tr (AA)

Citation: Bender O, Llorent-Martínez EJ, Zengin G, Mollica A, Ceylan R, Molina-García L, et al. (2018) Integration of *in vitro* and *in silico* perspectives to explain chemical characterization, biological potential and anticancer effects of *Hypericum salsugineum*: A pharmacologically active source for functional drug formulations. PLoS ONE 13(6): e0197815. https://doi.org/10.1371/journal.pone.0197815

Editor: Gabriel Agbor, Institute of Medical Research and Medicinal Plant Studies, CAMEROON

Received: December 25, 2017

Accepted: March 27, 2018

Published: June 4, 2018

Data Availability Statement: All relevant data are with the paper. There are no ethical or legal restrictions on sharing data sets.

Funding: The authors received no specific funding for this work.

Competing interests: The authors have declared that no competing interests exist.

Abstract

The genus *Hypericum* is one of the most popular genera in both traditional medicine and scientific platform. This study is designed to provide conceptual insights on the biological potential and chemical characterization of *H. salsugineum*, which is endemic to Turkey. The qualitative and quantitative phenolic content of the extracts was characterized by HPLC-ESI-MS^n. Biological efficiency was investigated by enzyme inhibitory assays (cholinesterases, tyrosinase, amylase, and glucosidase) and anti-cancer efficacy tests (anti-proliferative activities with the iCELLigence technology, colony formation and wound healing scratch assays). Phenolic acids (3-*O*-caffeoylquinic, 5-*O*-caffeoylquinic, and 4-*O*-caffeoylquinic acids) were the predominant group in the studied extracts, although several flavonoids were also detected and quantified. The extracts exhibited good inhibitory effects on tyrosinase and glucosidase, while they had weak ability against cholinesterases and amylase. Computational studies were also performed to explain the interactions between the major phenolics and these enzymes. The extracts displayed significant anti-cancer effects on breast carcinoma cell lines. Our findings suggest that *Hypericum salsugineum* could be valued as a potential source of biologically-active compounds for designing novel products.

Introduction

The plant kingdom usually presents high levels of polyphenols, which are known for their high biological properties such as antioxidant, antimicrobial, and anticancer. Hence, although the health benefits of phenolic compounds have been reported for decades, studies on this area are still a significant concern for many fields of research, including analytical chemistry, biochemistry, biomedicine, etc. Within this framework, uninvestigated wild plant species are also widely studied

to find new sources of valuable phytochemicals and, hence, to combat global health problems including cancer, Alzheimer disease, and diabetes mellitus. In many cases, researchers focus on plants commonly used in folk medicine. However, the information of these species is usually extensive, and focusing on less-known species from the same genus is an interesting option, as their composition and bio(chemical) activity may be similar. From this point, new studies could open further avenues in the design of potential phytopharmaceuticals.

The genus *Hypericum* (Hypericaceae) comprehends nearly 500 species which are widely distributed around the world. These species occur as herbs, shrubs and, infrequently trees. Among them, *H*. *perforatum* L. is the best-known species, used in traditional medicine and in the preparation of dietary supplements [1, 2]. Several authors have recently investigated potential medicinal applications of other *Hypericum* species, such as *H*. *androsaemum*, *H*. *connatum*, *H*. *olympicum*, and *H*. *adenotrichum*, among others [3–5], mainly studying their biological activity. Phenolic compounds usually account for many of the bio(chemical) properties of plant extracts, so exhaustive investigation of the phytochemical composition of the plant extracts is mandatory. Different phenolics have been reported in *Hypericum* species, including catechin, quercetin derivatives, phenolic acids, etc. [6, 7], each of these compounds presenting specific chemical properties. In this work, we aimed to study the phytochemical profile and bioactivity of *H*. *salsugineum* N. Robson & Hub.-Mor., an uncommon species in this genus, providing exhaustive information in order to propose an alternative source of bio-(active) phytochemicals.

Hypericum salsugineum Rabson & Hub.-Mor. is among the least studied *Hypericum* species. We have found only a small number of scientific reports regarding this species. To our knowledge, only a little information was provided concerning the phenolic composition (chlorogenic acid, kaemperol, myricetin, quercetin, and quercetin glycosides) [8] and antiherpetic activity [9] of this plant. Maltas et al. carried out more experiments and provided additional data regarding the antioxidant and antibacterial activity of *H*. *salsugineum*, among other *Hypericum* species [10]. This research aims to provide a complete study on this species to date, including identification and quantification of the main polyphenols, enzyme inhibitory assays, and evaluation of anti-cancer effects.

Materials and methods

Plant material

Aerial parts of *Hypericum salsugineum* were collected from Konya (Cihanbeyli-Gölyazı, 38˚ 28'31.08"N, 33˚ 7'36.74"E, 950 m) (at the flowering season in 2015 summer) and air dried at room temperature. Taxonomic identification was confirmed by the senior taxonomist Dr. Murad Aydın Sanda, from the Department of Biology, Selcuk University, Turkey. The dried aerial parts were ground to a fine powder (about 0.2 mm) using a laboratory mill. Then, the air-dried aerial parts (10 g) were macerated with 200 mL of methanol at room temperature (25˚C ± 1˚C) for 24 hours. The extracts were concentrated to dryness under vacuum at 40 ˚C by using a rotary evaporator and stored at + 4˚C in the dark until use.

For the collection of plants, no specific permits were required for the described field studies. For any locations/activities, no specific permissions were required. All locations where the plants were collected were not privately-owned or protected in any way and the field studies did not involve endangered or protected species.

Chemicals and reagents

All reagents and standards were of analytical reagent (AR) grade unless stated otherwise. We purchased all phenolic standards from Sigma-Aldrich (St. Louis, MO, USA), and prepared

individual stock solutions in ethanol (HPLC grade; Sigma). LC–MS grade acetonitrile (CH_3CN, 99%; LabScan; Dublin, Ireland) and ultrapure water (Milli-Q Waters purification system; Millipore; Milford, MA, USA) were used for the HPLC-MS analyses.

Chromatographic conditions

For HPLC analysis, 5 mg of dried extract was re-dissolved in 1 ml of methanol, filtered through 0.45 μm PTFE membrane filters, and ten μL of the solution was injected.

The HPLC system was an Agilent Series 1100, composed of a vacuum degasser, an auto-sampler, a binary pump, and a G1315B diode array detector (Agilent Technologies, Santa Clara, CA, USA). We used a reversed phase Luna Omega Polar C_{18} analytical column of 150 x 3.0 mm and 5 μm particle size (Phenomenex, Torrance, CA, USA) and a Polar C_{18} Security Guard cartridge (Phenomenex) of 4 x 3.0 mm. The best separation was achieved with a mobile phase of water-formic acid (100:0.1, v/v) and CH_3CN. The following program was used: a) initial mobile phase, 10% CH_3CN; b) linear increase from 10% to 25% CH_3CN (0–25 min); c) 25% CH_3CN (25–30 min); d) linear increase from 25% to 50% CH_3CN (30–40 min); e) linear increase from 50% to 100% CH_3CN (40–42 min); f) 100% CH_3CN (42–47 min). Then, CH_3CN percentage was returned to the initial mobile phase, with a 7 min stabilization time. The flow rate was 0.4 ml min^{-1}.

The HPLC system was connected to an ion trap mass spectrometer (Esquire 6000, Bruker Daltonics, Billerica, MA, USA) equipped with an electrospray interface. The scan range was set at m/z 100–1200 with a speed of 13,000 Da/s. The ESI conditions were: drying gas (N_2) flow rate and temperature, 10 mL/min and 365 ˚C; nebulizer gas (N_2) pressure, 50 psi; capillary voltage, 4500 V; capillary exit voltage, -117.3 V. We used the auto MS^n mode for the acquisition of MS^n data, with isolation width of 4.0 m/z, and fragmentation amplitude of 0.6 V (MS^n up to MS^4). Esquire control software and Data Analysis were used for data acquisition and data processing, respectively.

Quantification of polyphenols

Calibration curves (0.5–100 μg/ml in MeOH) were prepared using the corresponding analytical standards when available in our laboratory. In other cases, an appropriate analytical standard was selected: quercetin, apigenin and mirycetin for the corresponding glycosides; 3-*O*-caffeoylquinic acid for caffeoylquinic acids and derivatives; and p-coumaric acid for its derivative. The quantitation was carried out at 320 nm for phenolic acids and 350 nm for flavonoids, using peak area at the analytical signal in the corresponding UV chromatograms. Total individual phenolic content (TIPC) was defined as the sum of the quantified phenolic compounds.

Enzyme inhibitory effects

Anti-cholinesterases, anti-tyrosinase, anti-amylase, and anti-glucosidase effects were tested for detecting enzyme inhibitory effects. Detailed experimental procedures were given in the below:

For Cholinesterase (ChE) inhibitory activity assay: Sample solution (2 mg/mL; 50 μL) was mixed with DTNB (5,5-dithio-bis(2-nitrobenzoic) acid, Sigma, St. Louis, MO, USA) (125 μL) and AChE (acetylcholines-terase (Electric ell acetylcholinesterase, Type-VI-S, EC 3.1.1.7, Sigma)), or BChE (butyrylcholinesterase (horse serum butyrylcholinesterase, EC 3.1.1.8, Sigma)) solution (25 μL) in Tris–HCl buffer (pH 8.0) in a 96-well microplate and incubated for 15 min at 25 ˚C. The reaction was then initiated with the addition of acetylthiocholine iodide (ATCI, Sigma) or butyrylthiocholine chloride (BTCl, Sigma) (25 μL). Similarly, a blank was prepared by adding sample solution to all reaction reagents without enzyme (AChE or

BChE) solution. The sample and blank absorbances were read at 405 nm after 10 min incubation at 25 ˚C. The absorbance of the blank was subtracted from that of the sample and the cholinesterase inhibitory activity was expressed as galanthamine equivalents (mgGALAE/g extract) [11].

For Tyrosinase inhibitory activity assay: Sample solution (2 mg/mL; 25 μL) was mixed with tyrosinase solution (40 μL, Sigma) and phosphate buffer (100 μL, pH 6.8) in a 96-well microplate and incubated for 15 min at 25 ˚C. The reaction was then initiated with the addition of L-DOPA (40 μL, Sigma). Similarly, a blank was prepared by adding sample solution to all reaction reagents without enzyme (tyrosinase) solution. The sample and blank absorbances were read at 492 nm after a 10 min incubation at 25 ˚C. The absorbance of the blank was subtracted from that of the sample and the tyrosinase inhibitory activity was expressed as kojic acid equivalents (mgKAE/g extract) [12].

For α-amylase inhibitory activity assay: Sample solution (2 mg/mL; 25 μL) was mixed with α-amylase solution (ex-porcine pancreas, EC 3.2.1.1, Sigma) (50 μL) in phosphate buffer (pH 6.9 with 6 mM sodium chloride) in a 96-well microplate and incubated for 10 min at 37 ˚C. After pre-incubation, the reaction was initiated with the addition of starch solution (50 μL, 0.05%). Similarly, a blank was prepared by adding sample solution to all reaction reagents without enzyme (α-amylase) solution. The reaction mixture was incubated 10 min at 37 ˚C. The reaction was then stopped with the addition of HCl (25 μL, 1 M). This was followed by addition of the iodine-potassium iodide solution (100 μL). The sample and blank absorbances were read at 630 nm. The absorbance of the blank was subtracted from that of the sample and the α-amylase inhibitory activity was expressed as acarbose equivalents (mmol ACE/g extract) [13].

For α-glucosidase inhibitory activity assay: Sample solution (2 mg/mL; 50 μL) was mixed with glutathione (50 μL), α-glucosidase solution (from Saccharomyces cerevisiae, EC 3.2.1.20, Sigma) (50 μL) in phosphate buffer (pH 6.8) and PNPG (4-N-trophenyl-α-D-glucopyranoside, Sigma) (50 μL) in a 96-well microplate and incubated for 15 min at 37 ˚C. Similarly, a blank was prepared by adding sample solution to all reaction reagents without enzyme (α-glucosidase) solution. The reaction was then stopped with the addition of sodium carbonate (50 μL, 0.2 M). The sample and blank absorbances were read at 400 nm. The absorbance of the blank was subtracted from that of the sample and the α-glucosidase inhibitory activity was expressed as acarbose equivalents (mmol ACE/g extract) [14].

Molecular modelling

Enzymes preparation. For the computational studies, the following crystal structures have been downloaded from the Protein Data Bank RCSB PDB [15]: AChE (pdb:4X3C) [16] in complex with tacrine-nicotinamide hybrid inhibitor, BChE (pdb:4BDS) [17] in complex with tacrine, α-amylase (pdb:1VAH) [18] in complex with r-nitrophenyl-α-D-maltoside, α-glucosidase (pdb:3AXI) [19] in complex with maltose, and tyrosinase (pdb:2Y9X) [20] in complex with tropolone. The enzymes have been prepared for docking by removing the non-catalytic waters, the inhibitors, and all the other molecules present in the pdb files, as previously reported in our recent publications [11, 21–23]. The proteins were neutralized at pH 7.4 by PROPKA; seleno-cysteines, and seleno-methionines, if present, were converted respectively to cysteines and methionines. All the missing fragments and other errors present in the crystal structures were automatically solved by the Wizard Protein Preparation implemented in Maestro 10.2 suite [24]; the crystallographic ligands were used to generate the docking grid.

Ligands preparation. 3-*O*-caffeoylquinic acid, 4-*O*-caffeoylquinic acid, 5-*O*-caffeoylquinic acid, myricetin-*O*-glucoside, quercetin-3-*O*-glucoside, quercetin-3-*O*-galactoside,

quercetin-3-*O*-rhamnoside, myricetin, and quercetin were selected as representative compounds to carry out molecular docking studies because these are well known bioactive compounds and are well represented in the extracts of *H*. *salsugineum*. The chemical structures have been downloaded from Zinc database [25] or drawn by Chemdraw software, and used for molecular modelling experiments after preparation. The ligands were prepared by the LigPrep tool embedded in Maestro 10.2, neutralized at pH 7.4 by Epik, and minimized by force field OPLS3 [26].

Molecular docking. The performance of Glide XP to dock for ligand docking and scoring on the selected enzymes, was judged by its ability to reproduce the docking poses found of the crystallographic inhibitor. Thus, a series of self-docking experiments were performed previously to run the docking experiments, by preparing the native inhibitors by the Ligand Preparation tool as described above, and by docking them to the respective enzymes. Glide has shown to be largely able to perform a reliable docking for all the selected enzymes by producing a pose within maximum 1.5 Angstroms of RMSD calculated by comparing them with the crystallographic pose [27] Dockings of the selected substances have been performed for each selected enzyme employed for the *in vitro* enzymatic inhibition tests in this work. Glide [28] has been employed for the docking calculations by using the eXtra Precision scoring function for all the enzymes; the binding pocket was determined automatically by centering the grid on the crystallographic inhibitor, extended in a box of 20 Angstroms for each side. The best pose for each compound docked to the selected enzymes was the best ranked.

Cell lines and culture conditions

Human estrogen receptor-positive MCF-7 and triple negative MDA-MB-231 breast cancer cell lines were obtained from American Type Culture Collection (Rockville, Maryland, USA). Cells were maintained in Dulbecco's Modified Eagle's Medium (DMEM) (Lonza, Basel, Switzerland) supplemented with 10% heat-inactivated fetal bovine serum (FBS) (Biowest, Nuaillé, France), 2 mM L-glutamine, 100 U/ml penicillin, and 100 μg/ml streptomycin at 37˚C in a 5% CO_2 humidified incubator. Cells were routinely passaged every two to three days per week (1:3 ratio). When the cells reached 80% confluency, they were first washed with phosphate buffered saline (PBS), and then trypsinized with 0.25% trypsin-EDTA solution. Total cells were counted using trypan blue dye exclusion method on a hemocytometer before seeding on E-plate L8 or 6-well plate.

Cytotoxicity and anti-proliferative activity assay using the iCELLigence system

Dynamic monitoring of cytotoxicity and anti-proliferative activity were determined by using iCELLigence real-time cell analysis technology (ACEA Biosciences, San Diego, CA, USA) as previously described [29]. Briefly, after a background reading with 200 μl growth medium on iCELLigence E-plate L8, 100 μl of MCF-7 and MDA-MB-231 cells were seeded at a density of 5.0×10^4 per well. The system was then set to take impedance measurements every 30 min for 72 h. After culturing the cells for 24 h, they were treated with *H*. *salsugineum* methanolic extract between the range of 62.5–2000 μg/ml. The extract was dissolved in growth medium containing %0,1 DMSO for each experiment and all doses were prepared by serial dilution from a 2 mg/ml stock concentrate. In all experiments, %0,1 DMSO and %5 DMSO were used as negative control and positive controls, respectively. The data was recorded and analyzed by iCELLigence software integrated within the system. IC_{50} values (μg/ml) were calculated according to the values at the end of 72 h of all treatment doses. Each assay was performed in duplicate and the IC_{50} values shown are the average of at least three independent experiments.

Colony formation assay

Colony formation assay allows testing long-term effects of experimental therapeutics on cell colonies [30]. MCF-7 and MDA-MB-231 cells were plated into 6-well tissue culture plates (3.0 x 10^3 per well) and allowed to adhere for 24h. The cells were then treated with 62.5, 125, 250, and 350 μg/ml of *H. salsugineum* methanolic extract. %0,1 DMSO was used as control. Following treatment, plates were incubated for 14 days at 37˚C in 5% CO_2 humidified incubator. Next, the cells were gently washed with ice-cold PBS and fixed with MeOH:acetic acid (3:1, v:v) solution for 5 min at room temperature. Following removal of the fixative solution, they were stained with %0,05 crystal violet for 15 min at room temperature. The plates were washed with double-distilled water and left to dry overnight at room temperature. Colonies containing >50 cells were counted under a stereomicroscope Leica MZ16 A (Wetzlar, Germany).

Wound healing scratch assay

Wound healing assay is performed to test the migration ability of cells by measuring their motility [31]. MCF-7 and MDA-MB-231 cells were seeded in 6-well tissue culture plates at a density of 1.0 x 10^6 cells/well and cultured in growth medium for 24h. Then, the cells were scratched by a sterile 200 μl pipette tip. Cellular debris was removed and cells were washed with fresh growth medium gently. The cells were incubated with 350 μg/ml *H. salsugineum* methanolic extract for 48h. %0.1 DMSO was used as control. Wounded areas were photographed under an inverted microscope Leica DM IL LED (Wetzlar, Germany) at time points 0 and 48 h after scratching. Images were processed and quantified using the ImageJ software (National Institutes of Health, USA).

Statistical analysis

IC_{50} values were calculated using the iCELLigence software. IC_{50} values, colony formation, and wound closure rates are shown as means ± standard deviations (means ± SD). The statistical analyses were performed using the t-test to compare differences in results between the control and treatment groups. $P<0.05$ was considered to be statistically significant.

Results and discussion

HPLC-ESI-MS^n

We carried out the identification of phenolics (and other minor compounds) in *H.salsugineum* by HPLC-ESI-MS^n using negative ionization mode. Three independent solutions of the dried extract were analyzed, obtaining similar profiles (see characterization in Table 1). The base peak chromatogram of the methanolic extract of the plant is shown in Fig 1.

The initial step for the characterization of each compound consisted in the determination of its molecular weight: the base peak corresponded to the deprotonated molecular ion $[M-H]^-$, except for one formate adduct. For the identification of the flavonoid glycosides, we compared the mass spectra of the aglycones with analytical standards when available (apigenin, kaempferol, luteolin, and quercetin). Rutin and caffeoylquinic acids were identified by comparison with analytical standards. When reference compounds were not available, we compared the experimental spectra with data from scientific literature.

Phenolic acids. Four caffeoylquinic acids were present in the analyzed extracts. Compounds **4**, **6**, and **7** exhibited deprotonated molecular ions at m/z 353. We characterized them by comparison with analytical standards. Compounds **4** and **6**, with the typical 353→191 transition, corresponded to neochlorogenic acid (trans-5-*O*-caffeoylquinic acid) and chlorogenic acid (3-*O*-caffeoylquinic acid), respectively. Compound **7** presented MS^2[353] base peak at m/

Table 1. Characterization of methanol extract of *H. salsugineum*.

N°.	t_R (min)	$[M-H]^-$ *m/z*	m/z (% base peak)	Assigned identification
1	1.8	377	MS^2 [377]: 341 (100) MS^3 [377→341]: 179 (100), 161 (70), 131 (7), 119 (72)	Saccharide (derivative)
2	1.8	191	MS^2 [191]: 173 (20), 127 (12), 111 (100)	Quinic acid *
3	2.0	451	MS^2 [451]: 449 (48), 353 (100) MS^3 [451→353]: 191 (100), 179 (19), 173 (16), 135 (12)	Caffeoylquinic acid derivative
4	4.6	353	MS^2 [353]: 191 (100)	trans-5-*O*-caffeoylquinic acid *
5	7.0	337	MS^2 [337]: 163 (100) MS^3 [337→163]: 119 (100)	3-*p*-coumaroylquinic acid
6	7.5	353	MS^2 [353]: 191 (100)	3-*O*-caffeoylquinic acid *
7	8.0	353	MS^2 [353]: 191 (26), 179 (61), 173 (100) MS^3 [353→173]: 111 (100)	4-*O*-caffeoylquinic acid *
8	9.7	431	MS^2 [431]: 385 (100) MS^3 [431→385]: 223 (59), 205 (100), 161 (50), 153 (79)	Roseoside (formate adduct)
9	10.0	609	MS^2 [609]: 463 (69), 447 (88), 301 (100) MS^3 [609→301]: 271 (100), 179 (48), 151 (99)	Quercetin-*O*-hexoside-*O*-deoxyhexoside
10	11.4	337	MS^2 [337]: 173 (100), 191 (29) MS^3 [337→173]: 111 (100)	4-*p*-coumaroylquinic acid
11	12.2	371	MS^2 [371]: 249 (100), 231 (7) MS^3 [371→249]: 231 (54), 113 (100), 111 (38)	Unknown
12	12.8	367	MS^2 [367]: 191 (100), 173 (30) MS^3 [361→191]: 127 (100)	5-feruloylquinic acid
13	12.9	631	MS^2 [631]: 479 (100) MS^3 [631→479]: 317 (100), 316 (54), 179 (9) MS^4 [631→479→317]: 271 (100), 179 (72), 151 (55)	Myricetin-*O*-(*O*-galloyl)hexoside
14	14.7	479	MS^2 [479]: 317 (100), 316 (93) MS^3 [479→317]: 271 (100), 179 (83), 151 (65)	Myricetin-*O*-hexoside
15	15.1	367	MS^2 [367]: 191 (28), 179 (100), 135 (67) MS^3 [367→179]: 135 (100)	Methyl-caffeoyl-quinate
16	15.9	479	MS^2 [479]: 313 (100) MS^3 [479→313]: 241 (19), 169 (100), 125 (20)	Gallic acid derivative
17	16.3	593	MS^2 [593]: 503 (95), 485 (19), 473 (37), 413 (25), 383 (100) MS^3 [593→383]: 355 (100)	Vicenin-2*
18	16.5	521	MS^2 [521]: 359 (100) MS^3 [521→359]: 344 (100) MS^4 [521→359→344]: 329 (26), 313 (28), 300 (49), 189 (78), 159 (100)	Polymethoxylated flavonoid-*O*-hexoside
19	16.6	563	MS^2 [563]: 443 (8), 413 (100), 293 (85) MS^3 [563→413]: 293 (100) MS^4 [563→413→293]: 175 (100)	Apigenin-*C*-hexoside-*O*-pentoside
20	16.9	549	MS^2 [549]: 503 (100), 371 (45) MS^3 [549→503]: 371 (100), 161 (13) MS^4 [549→503→371]: 161 (100), 113 (17)	Unknown
21	17.0	641	MS^2 [641]: 479 (100), 317 (25) MS^3 [641→479]: 317 (100) MS^4 [641→479→317]: 179 (65), 151 (100)	Myricetin-*O*-dihexoside
22	17.7	609	MS^2 [609]: 301 (100), 300 (20) MS^3 [609→301]: 271 (100), 255 (54), 179 (51)	Rutin *
23	17.9	463	MS^2 [463]: 317 (76), 316 (100) MS^3 [463→316]: 271 (100), 179 (80), 151 (56)	Myricetin-*O*-deoxyhexoside
24	17.9	323	MS^2 [323]: 323 (100), 242 (51), 241 (24) MS^3 [323→242]: 240 (100), 172 (39)	Unknown
25	18.6	463	MS^2 [463]: 301 (100), 300 (20) MS^3 [463→301]: 179 (69), 151 (100)	Quercetin-*O*-hexoside

(*Continued*)

Table 1. (Continued)

N°.	t_R (min)	$[M-H]^-$ *m/z*	m/z (% base peak)	Assigned identification
26	19.2	463	MS^2 [463]: 301 (100) MS^3 [463→301]: 255 (21), 179 (79), 151 (100)	Quercetin-*O*-hexoside
27	19.5	415	MS^2 [415]: 225 (43), 179 (100), 161 (23), 149 (12) MS^3 [415→179]: 161 (100), 143 (24), 131 (44), 119 (44)	Saccharide (derivative)
28	20.4	517	MS^2 [517]: 209 (100)	Unknown
29	20.8	415	MS^2 [415]: 179 (100) MS^3 [415→179]: 161 (100), 143 (86), 131 (84), 119 (23)	Saccharide (derivative)
30	21.3	433	MS^2 [433]: 301 (100), 300 (70) MS^3 [433→301]: 271 (100), 255 (78), 179 (56), 151 (84)	Quercetin-*O*-pentoside
31	21.3	447	MS^2 [447]: 285 (100), 284 (96), 255 (21), 151 (7)	Kaempferol-*O*-hexoside
32	22.9	447	MS^2 [447]: 301 (100), 300 (17) MS^3 [447→301]: 179 (100), 151 (58)	Quercetin-*O*-deoxyhexoside
33	23.8	445	MS^2 [445]: 269 (100), MS^3 [445→269]: 225 (100)	Apigenin glucuronide
34	25.6	317	MS^2 [317]: 179 (100), 151 (38)	Myricetin
35	26.5	559	MS^2 [559]: 433 (100)	Unknown
36	27.0	431	MS^2 [431]: 285 (100) MS^3 [431→285]: 241 (100)	Luteolin-*O*-deoxyhexoside
37	27.3	625	MS^2 [625]: 479 (100), 317 (15), 316 (15) MS^3 [625→479]: 317 (91), 316 (100) MS^4 [625→479→316]: 271 (100), 179 (24), 151 (52)	Myricetin-*O*-deoxyhexoside-*O*-hexoside
38	29.4	523	MS^2 [523]: 313 (100) MS^3 [523→313]: 169 (100) MS^4 [523→313→169]: 125 (100)	Gallic acid derivative
39	30.4	543	MS^2 [543]: 417 (100)	Unknown
40	34.0	301	MS^2 [301]: 179 (71), 151 (100)	Quercetin *
41	35.5	547	MS^2 [547]: 313 (100) MS^3 [547→313]: 169 (100), 125 (25) MS^4 [547→313→169]: 125 (100)	Gallic acid derivative
42	38.6	327	MS^2 [327]: 291 (32), 229 (100), 211 (44), 171 (75)	Oxo-dihydroxy-octadecenoic acid
43	40.1	329	MS^2 [329]: 229 (76), 211 (100), 171 (39)	Trihydroxy-octadecenoic acid
44	41.0	537	MS^2 [537]: 443 (100), 417 (8), 385 (50), 151 (39)	Biflavone
45	42.1	537	MS^2 [537]: 443 (34), 417 (14), 399 (15), 375 (100) MS^3 [537→375]: 331 (100)	Amentoflavone

*Identified by comparison with analytical standards

https://doi.org/10.1371/journal.pone.0197815.t001

z 173, which is characteristic of 4-*O*-caffeoylquinic acid [32]. Compound **3** displayed MS^3 [451→353] base peak at m/z 191, so we characterized it as a caffeoylquinic acid derivative. Finally, compound **15**, with $[M-H]^-$ at m/z 367, was characterized as a methylated derivative according to bibliographic information [33].

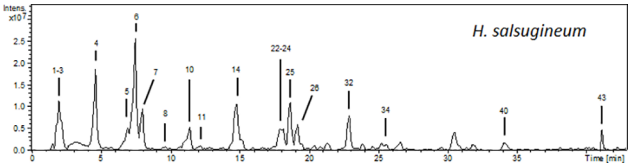

Fig 1. HPLC-ESI/MS^n base peak chromatogram (BPC) of the methanolic extract from *H. salsugineum*.

https://doi.org/10.1371/journal.pone.0197815.g001

We observed two coumaroylquinic acids and identified them according to the hierarchical scheme proposed by Clifford, Johnston (32). Both compounds (**5** and **10**) presented $[M-H]^-$ at m/z 337, but different fragmentations. Compound **5** corresponded to 3-*p*-coumaroylquinic acid (MS^2 base peak at m/z 163), whereas **10** was 4-*p*-coumaroylquinic acid (MS^2 base peak at m/z 173).

Compound **12** exhibited deprotonated molecular ion at m/z 367 and base peak at m/z 191, a fragmentation pattern that corresponds to 5-feruloylquinic acid [32].

We detected three gallic acid derivatives, compounds **16**, **38**, and **41** –all of them presented the characteristic 169→125 fragmentation of gallic acid–but a complete identification could not be carried out.

Flavonoids. A high number of the identified compounds were flavonoids, most of them *O*-glycosides, which we will classify by the aglycone. The identification of the attached moieties (sugars) to the aglycone was based on the observed neutral losses such as hexosyl (162 Da), deoxyhexosyl (146 Da), glucuronyl (176 Da), and pentosyl (132 Da).

Six quercetin glycosides were detected. Compound **40** corresponded to the aglycone (comparison with an analytical standard). Compound **9** suffered neutral losses of 162 Da and 146 Da, so it corresponded to quercetin-*O*-hexoside-*O*-deoxyhexoside. Compounds **25** and **26** were quercetin-*O*-hexoside isomers due to the loss of 162 Da. Similarly, we identified compounds **30** and **32** as quercetin-*O*-pentoside and quercetin-*O*-deoxyhexoside, respectively.

Five myricetin conjugates were characterized, with myricetin aglycone—$[M-H]^-$ at m/z 317 and characteristic fragment ions at m/z 179 and 151 –corresponding to compound **34**. Compound **13**, with a deprotonated molecular ion at m/z 631, suffered neutral losses of galloyl (152 Da) and hexosyl moieties 152 Da; it was myricetin-*O*-(*O*-galloyl)hexoside according to bibliography [34]. We characterized compound **14** as myricetin-*O*-hexoside, **21** as myricetin-*O*-dihexoside, **23** as myricetin-*O*-deoxyhexoside, and **37** as myricetin-*O*-deoxyhexoside-*O*-hexoside.

We detected three apigenin glycosides. Compound **17** presented deprotonated molecular ion at m/z 593, and its fragmentation pattern agreed with that of 6,8-di-*C*-glycosyl apigenin (vicenin-2) [35]. Compound **19**, with $[M-H]^-$ at m/z 563, presented fragment ions at m/z 413 and 293; we thus characterized it as an apigenin-*C*-hexoside-*O*-pentoside [36]. Finally, compound **33** displayed the neutral loss of 176 Da (glucuronide) to yield the aglycone at m/z 269, so we identified it as apigenin-*O*-glucuronide.

Compound **18** presented $[M-H]^-$ at m/z 521, and suffered neutral losses of hexosyl (521→359) and methoxyl (359→344, 344→329) moieties. This fragmentation pattern is consistent with polymethoxylated flavonoid hexosides.

Compound **31** and **36** corresponded to kaempferol-*O*-hexoside and luteolin-*O*-deoxyhexoside, respectively. The aglycones were characterized by comparison with analytical standards.

Finally, two biflavones were characterized. Compounds **43** and **45** presented the deprotonated molecular ions at m/z 537. On the one hand, the fragmentation pattern of compound **45** agreed with amentoflavone [37]. On the other hand, compound **44** was characterized as a biflavone, possibly biapigenin [38].

Other compounds. Compounds **1**, **27**, and **29** presented MS^n fragment ions at m/z 179, 161, 119, and 131, which have been previously reported in saccharides [39, 40]. We thus characterized these compounds as saccharides or saccharide derivatives.

Compound **8** was a formate adduct and presented the same fragmentation pattern than drovomifoliol-O-β-D-glucopyranoside, a terpenoid described by Li, Zhang [41], and reported as vomifoliol glucoside or roseoside by other authors [34].

We characterized tentatively compounds **42** and **43** as oxo-dihydroxy-octadecenoic and trihydroxy-octadecenoic acids, respectively, considering data from the scientific literature [42, 43].

Quantification of polyphenols

The concentrations of individual and total phenolics (TIPC) found in the analyzed extracts are shown in Table 2. It can be observed that phenolic acids represented the highest levels of phenolic compounds in *H. salsugineum* methanolic extract (approximately 80% of TIPC). The most abundant compounds were 3-*O*-caffeoylquinic acid (73 mg/g DE), 5-*O*-caffeoylquinic acid (51 mg/g DE) and a caffeoylquinic acid derivative (67 mg/g DE). The second most abundant group of compounds corresponded to flavonols, which were mainly composed of myricetin-*O*-hexoside (12.5 mg/g DE) and quercetin-*O*-hexoside isomers (19.2 mg/g DE). Finally, TIPC was 249 mg/g DE.

The concentrations of phenolic acids, as well as TIPC, compare favorably with the levels found in other *Hypericum* species. Jabeur, Tobaldini [44] reported a TIPC value of 110 mg/g in *H. androsaemum* extracts, approximately half the levels here observed. For 3-*O*-caffeoylquinic acid (3-CQA) and 5-*O*-caffeoylquinic acid, they observed concentrations of 11.6 and 40.1 mg/g extract, lower than the ones here observed. The levels of quercetin-*O*-hexoside isomers were similar in both cases. However, both the TIPC and phenolic acid concentrations reported in our studies are higher than those found in *H. androsaemum*. In *H. undulatum* [45], the levels of 3-CQA were also significantly lower (10–16 mg/g) than in the analyzed extracts of *H. salsugineum*. In *H. perforatum* shoots, only 3.1 mg/g of 3-CQA were reported [46], whereas quercetin hexoside and total flavonoid levels were also lower. Finally, 3-CQA levels in aerial parts of *H. origanifolium*, *H. montbretii*, and *H. perforatum* [47] were lower than the levels found in the present work, except for leaves of *H. montbretti*, which were 180 mg/g.

Table 2. Quantification of phenolic compounds in *H. salsugineum* (mg g^{-1} DE).

Nº.	Assigned identification	Concentration (mg g^{-1} DE)
Phenolic acids		
3 4	Caffeoylquinic acid derivative 5-*O*-caffeoylquinic acid	67 ± 4 51 ± 2
6	3-*O*-caffeoylquinic acid	73 ± 2
7	4-*O*-caffeoylquinic acid	10.5 ± 0.7
10	4-*p*-coumaroylquinic acid	5.1 ± 0.5
Total		**207 ± 5**
Flavonols		
14	Myricetin-*O*-hexoside	12.5 ± 0.9
25	Quercetin-*O*-hexoside	15.4 ± 0.8
26	Quercetin-*O*-hexoside	3.8 ± 0.3
32	Quercetin-*O*-deoxyhexoside	6.4 ± 0.3
34	Myricetin	0.83 ± 0.07
40	Quercetin	1.7 ± 0.1
Total		**41 ± 1**
Flavones		
33	Apigenin	0.3 ± 0.1
43	Biflavone	0.64 ± 0.05
Total		**0.9 ± 0.1**
TIPC		**249 ± 6**

https://doi.org/10.1371/journal.pone.0197815.t002

Enzyme inhibitory effects and molecular modelling

Natural enzyme inhibitors are gaining interest to combat global health problems including Alzheimer's disease, Diabetes mellitus, hyperpigmentation, and hypertension. The prevalence of these diseases is critically increasing worldwide, and thus effective strategies are required to control these diseases. With this in mind, the discovery of natural and safe enzyme inhibitors is one of the most investigated subjects in the scientific platform. For this purpose, we tested enzyme inhibitory effects of *H. salsugineum* extract against cholinesterase, tyrosinase, amylase, and glucosidase. The results are illustrated in Table 3. The tested extract possessed considerable inhibitory potential on tyrosinase and glucosidase. However, the extract exhibited weak ability on cholinesterases and amylase. Although several studies were performed on the enzyme inhibitory properties of some *Hypericum* species [48–50], this work provides the first information concerning *H. salsugineum*. The observed activity of the extract might be explained taking into account its phytochemical composition. Apparently, the phytochemical analysis of the extract evidenced the presence of several bioactive compounds. In this context, molecular docking was performed to understand possible interactions between phytochemicals and enzymes. The most abundant substances were selected as targets in the molecular modelling studies.

The best docking scores for all the selected substances docked into the enzymatic pocket of our enzyme pool are reported in Table 4. We focused the *in silico* experiments only on the most involved enzymes, namely α-glucosidase and tyrosinase. The analysis of the docking scores revealed that the best fitting on tyrosinase was given by the selected flavonols, and partially by the caffeoylquinic acids. We have found caffeoylquinic acid derivatives to give poor interactions with this enzyme by the leaving open to the hypothesis that isoquercitrin, quercetin, isoquercetin, and myricetin-3-*O*-glucoside may be responsible for the excellent inhibition activity found for the extract (Fig 2). Moreover, also the docking study on α-glucosidase, have shown the limited interaction of caffeoylquinic acids to the enzymatic pocket and high docking scores for quercetin, isoquercitrin, quercetin, and myricetin-3-*O*-glucoside (Fig 3). This observation is in agreement with the literature data which reports a good antidiabetic activity of several herbals extracts containing high amount of quercetin [51], isoquercitrin [52], myricetin [53, 54] and their glucosides, by the inhibition of α-glucosidase, and the inhibition of tyrosinase by isoquecitrin and isoquercetin [55, 56].

Evaluation of anti-cancer efficacy

Hypericum species are one of the most intensely studied groups in the research area of drug design and discovery of natural products for their effective pharmacological contents [57]. Many different *Hypericum* species' anti-neoplastic effects have been reported in various cancer

Table 3. Enzyme inhibitory effects of *H. salsugineum*.

Assays	Results
Acetylcholinesterase (mgGALAE/g)	1.689±0.150*
Butyrlcholinesterase (mgGALAE/g)	0.244±0.029
Tyrosinase (mgKAE/g)	65.29±0.41
α- Amylase (mmolACAE/g)	0.616±0.073
α-Glucosidase (mmolACAE/g)	19.466±0.704

*Values expressed are means ±S.D. of three parallel measurements. GALAE: Galantamine equivalent; KAE: Kojic acid equivalent; ACAE: Acarbose equivalent.

https://doi.org/10.1371/journal.pone.0197815.t003

Table 4. Docking scores obtained by Glide XP.

	α-Glucosidase	Tyrosinase
Compounds	**Docking Score**	**Docking Score**
Myricetin	-6.11	-6.898
Quercetin	-5.525	-6.959
3-*O*-caffeoylquinic a.	-7.147	-6.091
4-*O*-caffeoylquinic a.	-6.396	-6.698
5-*O*-caffeoylquinic a.	-8.034	-6.060
Myricetin-*O*-hexoside	-7.391	-9.221
Quercetin-*O*-hexoside	-8.221	-7.681
Quercetin	-5.384	-7.198
Isoquercitrin	-7.869	-8.290

https://doi.org/10.1371/journal.pone.0197815.t004

types, and specific phytochemical libraries were generated for new drug formulations [58–63]. In this study, anti-neoplastic effects of *H. salsugineum* were evaluated for the first time.

Breast cancer, which is a heterogeneous and complex disease, is the most common malignancy among women worldwide [64, 65]. Due to variable tissue and receptor activities, patients cannot benefit from the same treatment protocol. Although surgery, chemotherapy, and radiotherapy are the primary treatment modalities in breast cancer, hormone and targeted treatment options are being added according to the progression and type of the disease [66–71]. Despite all these advanced treatment options, efforts are underway to reduce the side effects of the drugs and to develop more effective agents. We investigated the effects of *H. salsugineum* on the cellular phenotype of cell lines for the two major molecular subtypes of breast cancer, luminal and basal. MCF-7 and MDA-MB-231, are well known for their clinical, pathological, and immunological characteristics, and are widely used model cell lines in breast cancer research [72]. MCF-7 is a luminal-type breast cancer cell line expressing estrogen receptor and MDA-MB-231 is basal-type cell line and has no hormone receptors such as estrogen receptor, progesterone receptor, and human epidermal growth factor receptor-2. MDA-MB-231 was also reported to be in the Claudin-low class during recent classification studies [73–75].

We initially investigated the time and dose-dependent effects of *H. salsugineum* methanolic extract on the cells by using a real-time, label-free iCELLigence cell analysis system. Platform measures the impedance via gold microelectrodes placed at the bottom of the system-specific E plate L8 and monitors the values in real time, resulting in quantitative high-throughput cellular data [76, 77]. In our study, cells were treated between the range of 62.5 and 2000 μg/ml of *H. salsugineum* extract and the effects were recorded in a total of 72 h. According to the obtained cell index values, cells were not viable following 2000 and 1000 μg/ml of *H. salsugineum* treatment, whereas an inhibition profile was observed between the range of 500 to 62,5 μg/ml treatments compared to the control (Fig 4). The IC50 values were calculated as 365.3±19.2 and 368±4.2 μg/ml for MCF-7 and MDA-MB-231, respectively. These results demonstrated that *H. salsugineum* displayed anti-proliferative effects on cells that were dynamically screened in a serial dose range and obtained IC50 values indicated that it was not cytotoxic to cells.

To observe the long-term effects of *H. salsugineum* on breast cancer cell lines, colony formation assay was performed. Based on the proliferation data, the cells were treated with doses close to and below the IC50 value of *H. salsugineum* extract for 14 days to determine the effect on the colony forming ability. Colony formation in both cell lines was significantly reduced with 62.5 and 125 μg/ml of *H. salsugineum* treatment and was completely inhibited with 250

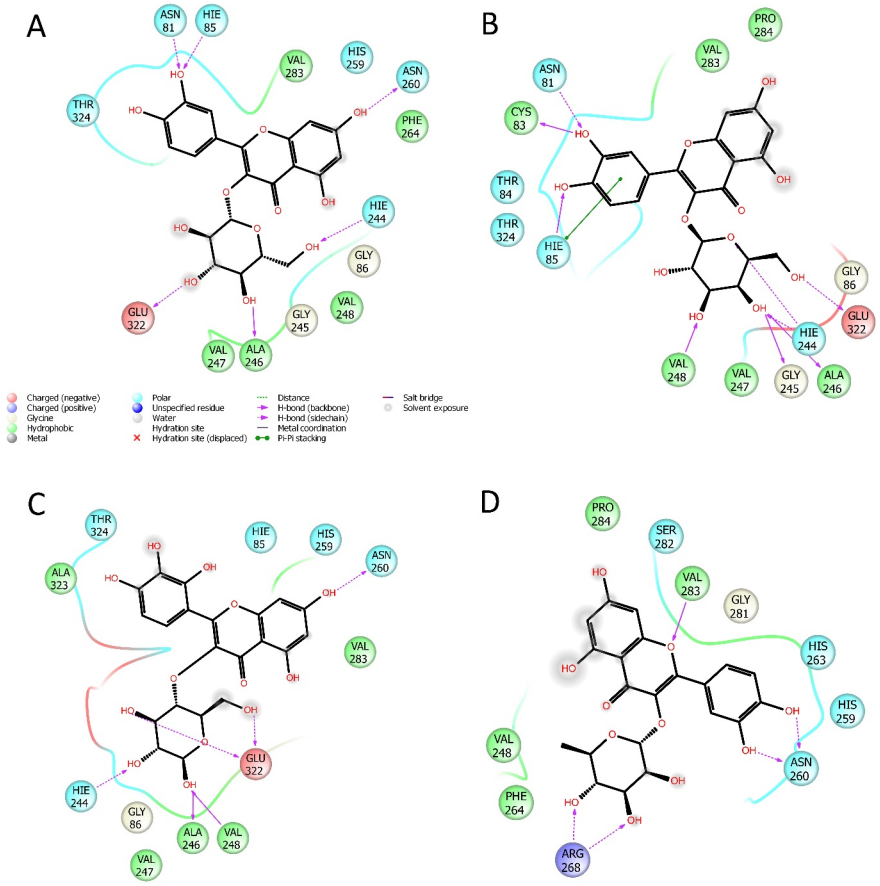

Fig 2. 2D representation of the best pose of (A) isoquercitrin, (B) isoquercetin, (C) myricetin-3-O-glucoside, (D) quercitrin docked in the catalitic pocket of tyrosinase.

https://doi.org/10.1371/journal.pone.0197815.g002

and 350 μg/ml of the extract. *H. salsugineum* was more effective on MCF-7 cells than MDA-MB-231 cells for inhibition of colony formation (Fig 5) which may be explained by the more invasive and metastatic characteristics of MDA-MB-231 cell line. However, at 350 μg /ml, which is close to the determined IC50 values, *H. salsugineum* displayed evident stochastic effects in both cell lines.

For observing the effects of *H. salsugineum* on the migration capabilities of MCF-7 and MDA-MB-231 cells, *in vitro* wound healing scratch assay was performed. Fig 6(A) shows the formed wounds at 0 h and the healing progression at 48 h. Cell migration was significantly reduced by 350 μg/ml *H. salsugineum* treatment in both cell lines, 21.06±3,9% in MCF-7 and 44.6±2,2% in MDA-MB-231, compared to control (Fig 6B and 6C). Similar to the results of colony formation assay, *H. salsugineum* was less effective in MDA-MB-231 cells in reducing the ability to migrate.

The results of our three consecutive assays -proliferation, colony formation, and wound healing- clearly confirmed that *H. salsugineum* significantly inhibited cellular growth in MCF-7 and MDA-MB-231 breast cancer cell lines. We believe that the inhibition effects of *H. salsugineum* on breast cancer cell lines are due to the compounds that we have identified (Table 2). *H. salsugineum* contains chlorogenic acid derivatives as major phenolic compounds, and myricetin and quercetin derivatives as major flavonols. All these phenolic compounds' chemopreventive properties and mechanisms of action are well-described in the literature [78].

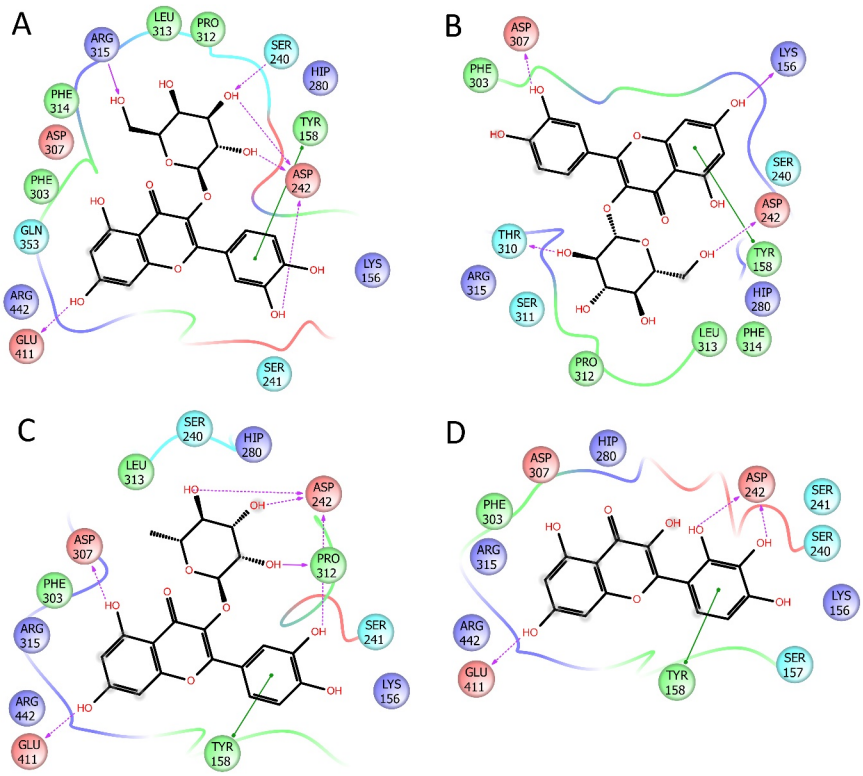

Fig 3. 2D representation of the best pose of (A) isoquercetin, (B) isoquercitrin, (C) quercitrin, (D) myricetin docked in the catalitic pocket of α-glucosidase.

https://doi.org/10.1371/journal.pone.0197815.g003

Focusing on recent breast cancer research, Jiao et al. reported that, myricetin suppressed the cell viability of MCF-7 cells mainly through p21-activated kinase 1 through downstream signaling of the β-catenin pathway [79]. In another study, Ranganathan et al. demonstrated that quercetin induces apoptosis in breast cancer cells through suppression of Twist via p38MAPK pathway [80]. Steiner, Davis [81] reported the dose-dependent positive effects of quercetin in transgenic mouse model of human breast cancer and identified the specific gene expression signature related to quercetin treatment. Chlorogenic acid, which is found in the human diet as one of the major active ingredients of many foods, was shown to suppress the proliferative and invasive phenotype of breast cancer cells [82–84]. The results of this study demonstrate that *H. salsugineum* methanolic extract has anti-cancer effects on the variable type of breast cancer cell lines with different comprehensive assays. Our findings and earlier research indicate that the inhibitory effects of *H. salsugineum* on breast cancer cells may be associated with these compounds and *H. salsugineum* can be used for new drug formulations with its bioactive content.

Conclusion

In recent years, biologically-active compounds have provided great potential as therapeutic agents to control significant health problems, such as Alzheimer's disease, type II diabetes, and cancer. Within the framework of this information, we focused on the biological potential and chemical characterization of *Hypericum salsugineum*. The tested extract possessed promising biological abilities with high levels of phenolic acids including 3-*O*-caffeoylquinic, 5-*O*-

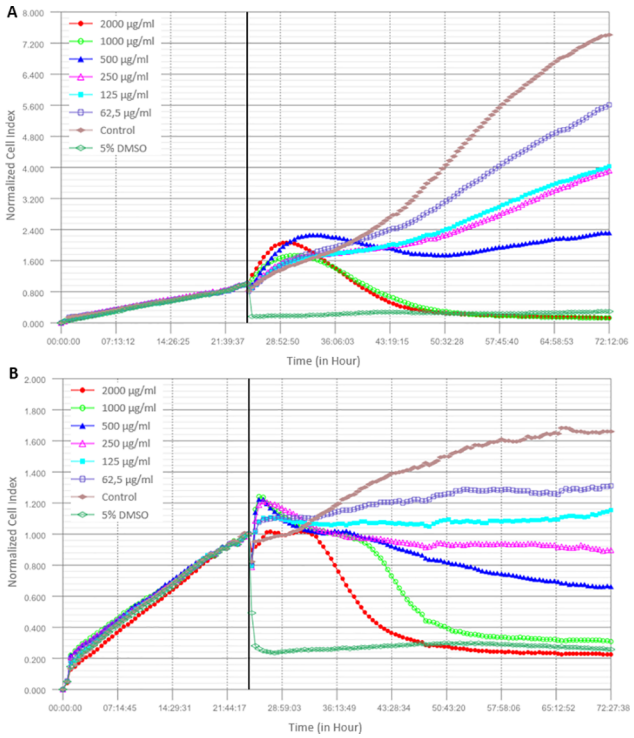

Fig 4. Anti-proliferative and cytotoxic effects of *H. salsugineum* methanolic extract on breast cancer cell lines via iCELLigence real time cell analysis system. (A) MCF-7 and (B) MDA-MB-231 cells were treated with varying concentrations (62,5 to 2000 µg/ml) of *H. salsugineum* methanolic extract. Charts were represented impedance measurements for 72h in real time and without any additional labelling. IC50 values are the means ± standard deviation of three independent experiments.

https://doi.org/10.1371/journal.pone.0197815.g004

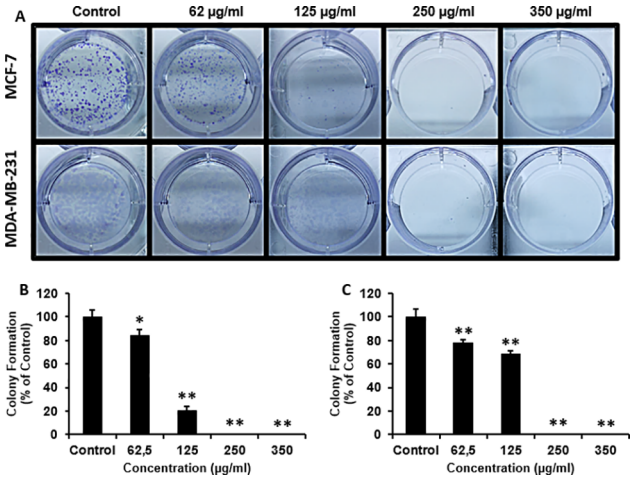

Fig 5. Colony formation ability of breast cancer cell lines by *H. salsugineum* methanolic extract treatment. (A) Representative images were showing colony formations for breast cancer cells which were treated with increasing concentrations (62,5 to 350 µg/ml) of *H. salsugineum* methanolic extract for 14 days. Histograms show the mean number of colonies in (B) MCF-7 and (C) MDA-MB-231. Values are the means ± standard deviation of three independent experiments. $P<0.05$ is considered as statistically significant. $^{*}P<0.05$, $^{**}P<0.01$ compared to control.

https://doi.org/10.1371/journal.pone.0197815.g005

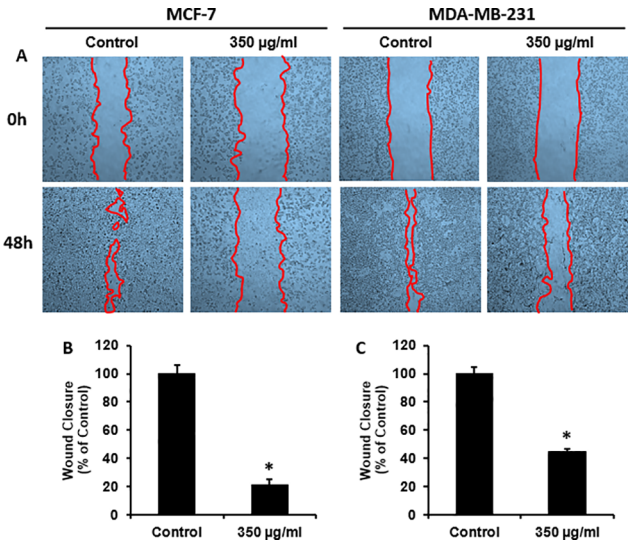

Fig 6. Inhibition of cell migration in breast cancer cell lines by wound healing assay after *H. salsugineum* methanolic extract treatment. Cells were scratched and treated with 350 µg/ml *H. salsugineum* methanolic extract for 48h. (A) Representative images were indicating wounded areas before and after treating of the cells. Closure rates were analyzed with ImageJ software. Bar graphs shows the mean of closure rates in (B) MCF-7 and (C) MDA-MB-231. The mean values and the ± standard deviation were obtained from three independent experiments. $P<0.05$ is considered as statistically significant. *$P<0.01$ compared to control.

https://doi.org/10.1371/journal.pone.0197815.g006

caffeoylquinic, and 4-*O*-caffeoylquinic acids. It significantly inhibited cellular growth in MCF-7 and MDA-MB-231 breast cancer cell lines. The current findings add to a growing body of literature on the genus *Hypericum* and the promising results here reported can provide a basis to design new phytopharmaceuticals and cosmeceuticals from *H. salsugineum*. However, further experimental studies (animal or bioavailability studies, etc.) into *H. salsugineum* are strongly recommended.

Author Contributions

Conceptualization: Onur Bender, Gokhan Zengin, Ramazan Ceylan.

Data curation: Onur Bender, Eulogio J. Llorent-Martínez, Gokhan Zengin, Adriano Mollica, Ramazan Ceylan.

Formal analysis: Onur Bender, Eulogio J. Llorent-Martínez, Gokhan Zengin, Adriano Mollica, Ramazan Ceylan, Lucia Molina-García, Maria Luisa Fernández-de Córdova, Arzu Atalay.

Methodology: Onur Bender, Eulogio J. Llorent-Martínez, Gokhan Zengin, Adriano Mollica, Ramazan Ceylan.

Resources: Eulogio J. Llorent-Martínez, Gokhan Zengin, Arzu Atalay.

Software: Adriano Mollica.

Supervision: Onur Bender, Gokhan Zengin, Arzu Atalay.

Validation: Onur Bender, Eulogio J. Llorent-Martínez, Gokhan Zengin, Adriano Mollica, Ramazan Ceylan, Lucia Molina-García, Maria Luisa Fernández-de Córdova, Arzu Atalay.

Visualization: Onur Bender, Eulogio J. Llorent-Martínez, Gokhan Zengin, Adriano Mollica.

Writing – original draft: Onur Bender, Eulogio J. Llorent-Martínez, Gokhan Zengin, Adriano Mollica, Ramazan Ceylan, Lucia Molina-García, Maria Luisa Fernández-de Córdova, Arzu Atalay.

Writing – review & editing: Eulogio J. Llorent-Martínez, Gokhan Zengin, Arzu Atalay.

References

1. Bruňáková K, Čellárová E. Conservation strategies in the genus *Hypericum* via cryogenic treatment. Frontiers in plant science. 2016; 7:558. https://doi.org/10.3389/fpls.2016.00558 PMID: 27200032
2. Crockett SL, Robson NK. Taxonomy and chemotaxonomy of the genus *Hypericum*. Medicinal and aromatic plant science and biotechnology. 2011; 5(Special Issue 1):1.
3. Antognoni F, Lianza M, Poli F, Buccioni M, Santinelli C, Caprioli G, et al. Polar extracts from the berry-like fruits of *Hypericum androsaemum* L. as a promising ingredient in skin care formulations. Journal of ethnopharmacology. 2017; 195:255–65. https://doi.org/10.1016/j.jep.2016.11.029 PMID: 27864112
4. Aztopal N, Erkisa M, Celikler S, Ulukaya E, Ari F. Antigrowth and apoptosis inducing effects of *Hypericum olympicum* L. and *Hypericum adenotrichum* Spach. on lung cancer cells in vitro: Involvement of DNA damage. Journal of Food Biochemistry. 2016; 40(4):559–66.
5. Scheggi S, Marandino A, Del Monte D, De Martino L, Pelliccia T, del Rosario Fusco M, et al. The protective effect of *Hypericum connatum* on stress-induced escape deficit in rat is related to its flavonoid content. Pharmaceutical biology. 2016; 54(9):1782–92. https://doi.org/10.3109/13880209.2015.1127979 PMID: 26731632
6. Jiang L, Numonov S, Bobakulov K, Qureshi MN, Zhao H, Aisa HA. Phytochemical Profiling and Evaluation of Pharmacological Activities of *Hypericum scabrum* L. Molecules. 2015; 20(6):11257–71. https://doi.org/10.3390/molecules200611257 PMID: 26096433
7. Sentkowska A, Biesaga M, Pyrzynska K. Effects of brewing process on phenolic compounds and antioxidant activity of herbs. Food Science and Biotechnology. 2016; 25(4):965–70.
8. Sakar M. Polyphenolic constituents of *Hypericum salsugineum*. Fitoterapia. 1990; 61(5).
9. Duman R. Antiherpetic activity of some endemic *Hypericum* species in Turkey. African Journal of Biotechnology. 2012; 11(5):1240–4.
10. Maltas E, Uysal A, Yildiztugay E, Aladag MO, Yildiz S, Kucukoduk M. Investigation of antioxidant and antibacterial activities of some *Hypericum* species. Fresenius Environ Bull. 2013; 22:862–9.
11. Mocan A, Zengin G, Crişan G, Mollica A. Enzymatic assays and molecular modeling studies of *Schisandra chinensis* lignans and phenolics from fruit and leaf extracts. Journal of enzyme inhibition and medicinal chemistry. 2016; 31(sup4):200–10. https://doi.org/10.1080/14756366.2016.1222585 PMID: 27595863
12. Mocan A, Zengin G, Simirgiotis M, Schafberg M, Mollica A, Vodnar DC, et al. Functional constituents of wild and cultivated Goji (*L. barbarum* L.) leaves: phytochemical characterization, biological profile, and computational studies. Journal of Enzyme Inhibition and Medicinal Chemistry. 2017; 32(1):153–68. https://doi.org/10.1080/14756366.2016.1243535 PMID: 28095717
13. Savran A, Zengin G, Aktumsek A, Mocan A, Glamoćlija J, Ćirić A, et al. Phenolic compounds and biological effects of edible *Rumex scutatus* and *Pseudosempervivum sempervivum*: potential sources of natural agents with health benefits. Food & function. 2016; 7(7):3252–62.
14. Llorent-Martínez E, Ortega-Barrales P, Zengin G, Uysal S, Ceylan R, Guler G, et al. *Lathyrus aureus* and *Lathyrus pratensis*: characterization of phytochemical profiles by liquid chromatography-mass spectrometry, and evaluation of their enzyme inhibitory and antioxidant activities. RSC Advances. 2016; 6(92):88996–9006.
15. Berman HM, Westbrook J, Feng Z, Gilliland G, Bhat TN, Weissig H, et al. The protein data bank. Nucleic acids research. 2000; 28(1):235–42. PMID: 10592235
16. Pesaresi A, Lamba D. Torpedo Californica Acetylcholinesterase In Complex With A Tacrine-Nicotinamide Hybrid Inhibitor.
17. Nachon F, Carletti E, Ronco C, Trovaslet M, Nicolet Y, Jean L, et al. Crystal structures of human cholinesterases in complex with huprine W and tacrine: elements of specificity for anti-Alzheimer's drugs targeting acetyl-and butyryl-cholinesterase. Biochemical Journal. 2013; 453(3):393–9. https://doi.org/10.1042/BJ20130013 PMID: 23679855
18. Zhuo H, Payan F, Qian M. Crystal structure of the pig pancreatic α-amylase complexed with ρ-nitrophenyl-α-d-maltoside-flexibility in the active site. The protein journal. 2004; 23(6):379–87. PMID: 15517985

19. Yamamoto K, Miyake H, Kusunoki M, Osaki S. Steric hindrance by 2 amino acid residues determines the substrate specificity of isomaltase from *Saccharomyces cerevisiae*. Journal of bioscience and bioengineering. 2011; 112(6):545–50. https://doi.org/10.1016/j.jbiosc.2011.08.016 PMID: 21925939

20. Ismaya WT, Rozeboom HJ, Weijn A, Mes JJ, Fusetti F, Wichers HJ, et al. Crystal structure of Agaricus bisporus mushroom tyrosinase: Identity of the tetramer subunits and interaction with tropolone. Biochemistry. 2011; 50(24):5477–86. https://doi.org/10.1021/bi200395t PMID: 21598903

21. Mocan A, Zengin G, Uysal A, Gunes E, Mollica A, Degirmenci NS, et al. Biological and chemical insights of *Morina persica* L.: A source of bioactive compounds with multifunctional properties. Journal of Functional Foods. 2016; 25:94–109.

22. Zengin G, Ceylan R, Katanić J, Mollica A, Aktumsek A, Boroja T, et al. Combining in vitro, in vivo and in silico approaches to evaluate nutraceutical potentials and chemical fingerprints of *Moltkia aurea* and *Moltkia coerulea*. Food and Chemical Toxicology. 2017.

23. Zengin G, Uysal A, Aktumsek A, Mocan A, Mollica A, Locatelli M, et al. *Euphorbia denticulata* Lam.: A promising source of phyto-pharmaceuticals for the development of novel functional formulations. Biomedicine & Pharmacotherapy. 2017; 87:27–36.

24. Maestro S. Version 9.2. LLC, New York. 2011.

25. Irwin JJ, Sterling T, Mysinger MM, Bolstad ES, Coleman RG. ZINC: a free tool to discover chemistry for biology. Journal of chemical information and modeling. 2012; 52(7):1757–68. https://doi.org/10.1021/ci3001277 PMID: 22587354

26. Shelley JC, Cholleti A, Frye LL, Greenwood JR, Timlin MR, Uchimaya M. Epik: a software program for pK a prediction and protonation state generation for drug-like molecules. Journal of computer-aided molecular design. 2007; 21(12):681–91. https://doi.org/10.1007/s10822-007-9133-z PMID: 17899391

27. Hevener KE, Zhao W, Ball DM, Babaoglu K, Qi J, White SW, et al. Validation of molecular docking programs for virtual screening against dihydropteroate synthase. Journal of chemical information and modeling. 2009; 49(2):444–60. https://doi.org/10.1021/ci800293n PMID: 19434845

28. Friesner RA, Murphy RB, Repasky MP, Frye LL, Greenwood JR, Halgren TA, et al. Extra precision glide: docking and scoring incorporating a model of hydrophobic enclosure for protein-ligand complexes. Journal of medicinal chemistry. 2006; 49(21):6177–96. https://doi.org/10.1021/jm051256o PMID: 17034125

29. Picot MCN, Bender O, Atalay A, Zengin G, Loffredo L, Hadji-Minaglou F, et al. Multiple pharmacological targets, cytotoxicity, and phytochemical profile of *Aphloia theiformis* (Vahl.) Benn. Biomedicine & Pharmacotherapy. 2017; 89:342–50.

30. Franken NA, Rodermond HM, Stap J, Haveman J, Van Bree C. Clonogenic assay of cells in vitro. Nature protocols. 2006; 1(5):2315. https://doi.org/10.1038/nprot.2006.339 PMID: 17406473

31. Liang C-C, Park AY, Guan J-L. In vitro scratch assay: a convenient and inexpensive method for analysis of cell migration in vitro. Nature protocols. 2007; 2(2):329–33. https://doi.org/10.1038/nprot.2007.30 PMID: 17406593

32. Clifford MN, Johnston KL, Knight S, Kuhnert N. Hierarchical scheme for LC-MS n identification of chlorogenic acids. Journal of Agricultural and Food Chemistry. 2003; 51(10):2900–11. https://doi.org/10.1021/jf026187q PMID: 12720369

33. Simirgiotis MJ. Antioxidant capacity and HPLC-DAD-MS profiling of Chilean Peumo (Cryptocarya alba) fruits and comparison with German Peumo *(Crataegus monogyna*) from Southern Chile. Molecules. 2013; 18(2):2061–80. https://doi.org/10.3390/molecules18022061 PMID: 23385342

34. Spínola V, Llorent-Martínez EJ, Gouveia S, Castilho PC. Myrica faya: A new source of antioxidant phytochemicals. Journal of agricultural and food chemistry. 2014; 62(40):9722–35. https://doi.org/10.1021/jf503540s PMID: 25266067

35. Ferreres F, Silva BM, Andrade PB, Seabra RM, Ferreira MA. Approach to the study of C-glycosyl flavones by ion trap HPLC-PAD-ESI/MS/MS: application to seeds of quince (*Cydonia oblonga*). Phytochemical Analysis. 2003; 14(6):352–9. https://doi.org/10.1002/pca.727 PMID: 14667061

36. Santos J, Oliveira M, Ibanez E, Herrero M. Phenolic profile evolution of different ready-to-eat baby-leaf vegetables during storage. Journal of Chromatography A. 2014; 1327:118–31. https://doi.org/10.1016/j.chroma.2013.12.085 PMID: 24438834

37. Wang J, Liu S, Ma B, Chen L, Song F, Liu Z, et al. Rapid screening and detection of XOD inhibitors from *S. tamariscina* by ultrafiltration LC-PDA–ESI-MS combined with HPCCC. Analytical and bioanalytical chemistry. 2014; 406(28):7379–87. https://doi.org/10.1007/s00216-014-8132-x PMID: 25240932

38. Zhang Y, Liu C, Zhang Z, Wang J, Wu G, Li S. Comprehensive separation and identification of chemical constituents from *Apocynum venetum* leaves by high-performance counter-current chromatography and high performance liquid chromatography coupled with mass spectrometry. Journal of Chromatography B. 2010; 878(30):3149–55.

39. Brudzynski K, Miotto D. Honey melanoidins: Analysis of the compositions of the high molecular weight melanoidins exhibiting radical-scavenging activity. Food Chemistry. 2011; 127(3):1023–30. https://doi.org/10.1016/j.foodchem.2011.01.075 PMID: 25214092

40. Verardo G, Duse I, Callea A. Analysis of underivatized oligosaccharides by liquid chromatography/electrospray ionization tandem mass spectrometry with post-column addition of formic acid. Rapid communications in mass spectrometry. 2009; 23(11):1607–18. https://doi.org/10.1002/rcm.4047 PMID: 19408275

41. Li X, Zhang Y, Zeng X, Yang L, Deng Y. Chemical profiling of bioactive constituents in Sarcandra glabra and its preparations using ultra-high-pressure liquid chromatography coupled with LTQ Orbitrap mass spectrometry. Rapid Communications in Mass Spectrometry. 2011; 25(17):2439–47. https://doi.org/10.1002/rcm.5123 PMID: 21818803

42. Levandi T, Püssa T, Vaher M, Toomik P, Kaljurand M. Oxidation products of free polyunsaturated fatty acids in wheat varieties. European journal of lipid science and technology. 2009; 111(7):715–22.

43. Van Hoyweghen L, De Bosscher K, Haegeman G, Deforce D, Heyerick A. In Vitro Inhibition of the Transcription Factor NF-κB and Cyclooxygenase by Bamboo Extracts. Phytotherapy Research. 2014; 28 (2):224–30. https://doi.org/10.1002/ptr.4978 PMID: 23559516

44. Jabeur I, Tobaldini F, Martins N, Barros L, Martins I, Calhelha RC, et al. Bioactive properties and functional constituents of *Hypericum androsaemum* L.: A focus on the phenolic profile. Food Research International. 2016; 89:422–31. https://doi.org/10.1016/j.foodres.2016.08.040 PMID: 28460934

45. Rainha N, Koci K, Coelho AV, Lima E, Baptista J, Fernandes-Ferreira M. HPLC–UV–ESI-MS analysis of phenolic compounds and antioxidant properties of *Hypericum undulatum* shoot cultures and wild-growing plants. Phytochemistry. 2013; 86:83–91. https://doi.org/10.1016/j.phytochem.2012.10.006 PMID: 23141168

46. Tusevski O, Stanoeva JP, Stefova M, Pavokovic D, Simic SG. Identification and quantification of phenolic compounds in *Hypericum perforatum* L. transgenic shoots. Acta physiologiae plantarum. 2014; 36 (10):2555–69.

47. Öztürk N, Tunçel M, Potoğlu-Erkara İ. Phenolic compounds and antioxidant activities of some *Hypericum* species: A comparative study with *H. perforatum*. Pharmaceutical biology. 2009; 47(2):120–7.

48. Bejaoui A, Ben Salem I, Rokbeni N, M'Rabet Y, Boussaid M, Boulila A. Bioactive compounds from *Hypericum humifusum* and *Hypericum perfoliatum*: inhibition potential of polyphenols with acetylcholinesterase and key enzymes linked to type-2 diabetes. Pharmaceutical Biology. 2017; 55(1):906–11. https://doi.org/10.1080/13880209.2016.1270973 PubMed PMID: WOS:000395131900019. PMID: 28147885

49. Mandrone M, Lorenzi B, Venditti A, Guarcini L, Bianco A, Sanna C, et al. Antioxidant and anti-collagenase activity of *Hypericum hircinum* L. Industrial Crops and Products. 2015; 76:402–8. https://doi.org/10.1016/j.indcrop.2015.07.012 PubMed PMID: WOS:000364890600050.

50. Zheleva-Dimitrova D, Nedialkov P, Momekov G. Benzophenones from *Hypericum elegans* with antioxidant and acetylcholinesterase inhibitory potential. Pharmacognosy Magazine. 2013; 9(36):1–5. https://doi.org/10.4103/0973-1296.117846 PubMed PMID: WOS:000330987200001. PMID: 24143038

51. Kumar S, Narwal S, Kumar V, Prakash O. α-glucosidase inhibitors from plants: A natural approach to treat diabetes. Pharmacognosy reviews. 2011; 5(9):19. https://doi.org/10.4103/0973-7847.79096 PMID: 22096315

52. Lobo JFR, Vinther JM, Borges RM, Staerk D. High-resolution α-glucosidase inhibition profiling combined with HPLC-HRMS-SPE-NMR for identification of antidiabetic compounds in *Eremanthus crotonoides* (Asteraceae). Molecules. 2016; 21(6):782.

53. Kang S-J, Park J-HY, Choi H-N, Kim J-I. α-glucosidase inhibitory activities of myricetin in animal models of diabetes mellitus. Food Science and Biotechnology. 2015; 24(5):1897–900.

54. Meng Y, Su A, Yuan S, Zhao H, Tan S, Hu C, et al. Evaluation of total flavonoids, myricetin, and quercetin from *Hovenia dulcis* Thunb. As inhibitors of α-amylase and α-glucosidase. Plant Foods for Human Nutrition. 2016; 71(4):444–9. https://doi.org/10.1007/s11130-016-0581-2 PMID: 27787697

55. Arung ET, Furuta S, Ishikawa H, Tanaka H, Shimizu K. Melanin Biosynthesis Inhibitory and Antioxidant Activities of Quercetin-3'-O-β-D-glucoside Isolated from *Allium cepa*. Zeitschrift für Naturforschung C. 2011; 66(5–6):209–14.

56. de Freitas MM, Fontes PR, Souza PM, Fagg CW, Guerra ENS, de Medeiros Nóbrega YK, et al. Extracts of *morus nigra* l. Leaves standardized in chlorogenic acid, rutin and isoquercitrin: Tyrosinase inhibition and cytotoxicity. PloS one. 2016; 11(9):e0163130. https://doi.org/10.1371/journal.pone.0163130 PMID: 27655047

57. Wölfle U, Seelinger G, Schempp CM. Topical application of St. John's wort (Hypericum perforatum). Planta medica. 2014; 80(02/03):109–20.

58. Haefeli WE, Carls A. Drug interactions with phytotherapeutics in oncology. Expert opinion on drug metabolism & toxicology. 2014; 10(3):359–77.
59. Kleemann B, Loos B, Scriba TJ, Lang D, Davids LM. St John's Wort (*Hypericum perforatum* L.) photomedicine: Hypericin-photodynamic therapy induces metastatic melanoma cell death. PloS one. 2014; 9 (7):e103762. https://doi.org/10.1371/journal.pone.0103762 PMID: 25076130
60. Madunić J, Matulić M, Friščić M, Pilepić KH. Evaluation of the cytotoxic activity of *Hypericum* spp. on human glioblastoma A1235 and breast cancer MDA MB-231 cells. Journal of Environmental Science and Health, Part A. 2016; 51(13):1157–63.
61. Sarimahmut M, Balikci N, Celikler S, Ari F, Ulukaya E, Guleryuz G, et al. Evaluation of genotoxic and apoptotic potential of *Hypericum adenotrichum* Spach. in vitro. Regulatory Toxicology and Pharmacology. 2016; 74:137–46. https://doi.org/10.1016/j.yrtph.2015.11.010 PMID: 26617407
62. Xavier CP, Lima CF, Fernandes-Ferreira M, Pereira-Wilson C. *Hypericum androsaemum* water extract inhibits proliferation in human colorectal cancer cells through effects on MAP kinases and PI3K/Akt pathway. Food & function. 2012; 3(8):844–52.
63. Zhao J, Liu W, Wang JC. Recent advances regarding constituents and bioactivities of plants from the genus Hypericum. Chemistry & biodiversity. 2015; 12(3):309–49.
64. Ferlay J, Soerjomataram I, Dikshit R, Eser S, Mathers C, Rebelo M, et al. Cancer incidence and mortality worldwide: sources, methods and major patterns in GLOBOCAN 2012. International journal of cancer. 2015; 136(5).
65. Torre LA, Bray F, Siegel RL, Ferlay J, Lortet-Tieulent J, Jemal A. Global cancer statistics, 2012. CA: a cancer journal for clinicians. 2015; 65(2):87–108.
66. Bange J, Zwick E, Ullrich A. Molecular targets for breast cancer therapy and prevention. Nature medicine. 2001; 7(5):548. https://doi.org/10.1038/87872 PMID: 11329054
67. Collaborators MWS. Breast cancer and hormone-replacement therapy in the Million Women Study. The Lancet. 2003; 362(9382):419–27.
68. Group EBCTC. Effects of chemotherapy and hormonal therapy for early breast cancer on recurrence and 15-year survival: an overview of the randomised trials. The Lancet. 2005; 365(9472):1687–717.
69. Lehmann BD, Bauer JA, Chen X, Sanders ME, Chakravarthy AB, Shyr Y, et al. Identification of human triple-negative breast cancer subtypes and preclinical models for selection of targeted therapies. The Journal of clinical investigation. 2011; 121(7):2750. https://doi.org/10.1172/JCI45014 PMID: 21633166
70. Polyak K. Heterogeneity in breast cancer. The Journal of clinical investigation. 2011; 121(10):3786. https://doi.org/10.1172/JCI60534 PMID: 21965334
71. Shao W, Brown M. Advances in estrogen receptor biology: prospects for improvements in targeted breast cancer therapy. Breast Cancer Research. 2003; 6(1):39. https://doi.org/10.1186/bcr742 PMID: 14680484
72. Holliday DL, Speirs V. Choosing the right cell line for breast cancer research. Breast cancer research. 2011; 13(4):215. https://doi.org/10.1186/bcr2889 PMID: 21884641
73. Neve RM, Chin K, Fridlyand J, Yeh J, Baehner FL, Fevr T, et al. A collection of breast cancer cell lines for the study of functionally distinct cancer subtypes. Cancer cell. 2006; 10(6):515–27. https://doi.org/10.1016/j.ccr.2006.10.008 PMID: 17157791
74. Perou CM, Sorlie T, Eisen MB, Van De Rijn M. Molecular portraits of human breast tumours. nature. 2000; 406(6797):747. https://doi.org/10.1038/35021093 PMID: 10963602
75. Sabatier R, Finetti P, Guille A, Adelaide J, Chaffanet M, Viens P, et al. Claudin-low breast cancers: clinical, pathological, molecular and prognostic characterization. Molecular cancer. 2014; 13(1):228.
76. Bird C, Kirstein S. Real-time, label-free monitoring of cellular invasion and migration with the xCELLigence system. Nature methods. 2009; 6(8).
77. Ke N, Wang X, Xu X, Abassi YA. The xCELLigence system for real-time and label-free monitoring of cell viability. Mammalian Cell Viability: Methods and Protocols. 2011:33–43.
78. Siddiqui JA, Singh A, Chagtoo M, Singh N, Godbole MM, Chakravarti B. Phytochemicals for breast cancer therapy: current status and future implications. Current cancer drug targets. 2015; 15(2):116–35. Epub 2014/12/30. PMID: 25544650.
79. Jiao D, Zhang XD. Myricetin suppresses p21-activated kinase 1 in human breast cancer MCF-7 cells through downstream signaling of the β-catenin pathway. Oncology reports. 2016; 36(1):342–8. https://doi.org/10.3892/or.2016.4777 PMID: 27122002
80. Ranganathan S, Halagowder D, Sivasithambaram ND. Quercetin suppresses twist to induce apoptosis in MCF-7 breast cancer cells. PloS one. 2015; 10(10):e0141370. https://doi.org/10.1371/journal.pone.0141370 PMID: 26491966

81. Steiner J, Davis J, McClellan J, Enos R, Carson J, Fayad R, et al. Dose-dependent benefits of quercetin on tumorigenesis in the C3 (1)/SV40Tag transgenic mouse model of breast cancer. Cancer biology & therapy. 2014; 15(11):1456–67.

82. Mileo AM, Di Venere D, Linsalata V, Fraioli R, Miccadei S. Artichoke polyphenols induce apoptosis and decrease the invasive potential of the human breast cancer cell line MDA-MB231. Journal of cellular physiology. 2012; 227(9):3301–9. https://doi.org/10.1002/jcp.24029 PMID: 22170094

83. Noratto G, Porter W, Byrne D, Cisneros-Zevallos L. Identifying peach and plum polyphenols with chemopreventive potential against estrogen-independent breast cancer cells. Journal of agricultural and food chemistry. 2009; 57(12):5219–26. https://doi.org/10.1021/jf900259m PMID: 19530711

84. Zhang L, Liu R, Niu W. Phytochemical and antiproliferative activity of proso millet. PloS one. 2014; 9(8): e104058. https://doi.org/10.1371/journal.pone.0104058 PMID: 25098952